

2D gel permeation chromatography (2D GPC) correlation studies of the growth process for perfluoro-octyltriethoxysilane polymer aggregates

Kenichi Izawa,^a Toshiaki Ogasawara,^b Hideki Masuda,^c Hirofumi Okabayashi,^{*c} Charmian J. O'Connor^d and Isao Noda^e

^a *Fuji Silysia Chemical Ltd., Nakatsugawa Technical Center, 1683-1880, Nakagaito, Nakatsugawa, Gifu 509-9132, Japan*

^b *Tokai Technical Center Foundation, 710, Inokoshi 2, Meito-ku, Nagoya, Aichi 465-0021, Japan*

^c *Department of Applied Chemistry, Nagoya Institute of Technology, Gokiso-cho, Showa-ku, Nagoya, Aichi 466-8555, Japan*

^d *Department of Chemistry, The University of Auckland, Private Bag 92019, Auckland, New Zealand*

^e *The Procter and Gamble Company 8611, Beckett Road, West Chester, OH 45069, USA*

Received 21st August 2001, Accepted 11th December 2001

First published as an Advance Article on the web 13th February 2002

A novel analytical technique, two-dimensional correlation gel permeation chromatography (2D correlation GPC), has been used to elucidate intricate details of the two-step (I and II) polymerization of 1*H*,1*H*,2*H*,2*H*-perfluoro-octyltriethoxysilane (PFOTES) catalyzed by 0.5, 1.0 and 2.0 M HCl-H₂O over a time period of 600–14 400 s. The 2D GPC correlation results demonstrate that each elution band (particularly, in step II) consists of two (reactive and nonreactive) components and that a higher HCl concentration enhances the correlation of the reactive component with other bands. It is suggested that rapid growth of the polymeric aggregates in step II may be caused by the appearance of these reactive components.

Introduction

The condensation reaction of alkoxides or alkylalkoxides has been extensively applied from sol-gel research to applications in industry.^{1–6} The reaction involves various intermediates or precursors, although the presence of these species in solution is very dependent upon reaction conditions. Therefore, elucidation of the nature of these species should have potential for further advancement in various applications.

Previous studies^{7,8} have observed time-resolved SAXS and near-IR spectra for reaction mixtures in a perfluoro-octyltriethoxysilane (PFOTES)–ethanol–HCl–H₂O system. The results, based on the time-dependence of the apparent radius of gyration and on the time-dependent near-IR data, provided a qualitative model of the growth process for the polymeric aggregates. This growth model may be summarized as follows. (1) The growth of polymeric aggregates proceeds in a two-step process, in which formation of small aggregates occurs in the initial step (step I), while, in the second step (step II), larger polymeric aggregates are rapidly produced prior to phase separation. (2) A higher HCl concentration increases the time for commencement of the second step.

A small-angle X-ray scattering (SAXS) study on the *n*-octyltriethoxysilane (OTES)–ethanol–HCl–H₂O system has also been carried out.⁷ The results led to the conclusion that growth of the OTES precursors occurs in two steps but on a shorter time scale, compared with that for the PFOTES system.

In a previous study,⁹ we suggested, for the first time, that the generalized two-dimensional (2D) correlation theory¹⁰ could be applied to three time-resolved gel permeation chromatography (GPC) elution profiles, and specifically to aliquots sampled in the initial 10 min from the reaction mixture of

the OTES–ethanol–1.0 M HCl–H₂O system. However, there were too few GPC elution profiles to be able to apply the 2D GPC correlation spectra to a detailed discussion of the reaction mechanism.

In a further 2D correlation GPC study,¹¹ we concluded that the synchronous and asynchronous correlation spectral features, which were calculated from ten sets of traces of time-dependent GPC profiles for the same reaction system sampled in the time range 60–540 s, directly reflected the reaction mechanism in the first stage of the polymerization process, thus demonstrating the promising potential of this technique. However, it should be emphasized that these correlation spectra did not provide sufficient evidence that the elution bands split into high (H)- and low (L)-elution components which have the potential to play a significant role in the reaction mechanism.

In this present study, time-resolved GPC and 2D correlation analyses have been used to examine further details of the two-step growth of polymeric aggregates in the PFOTES–ethanol–HCl–H₂O system, over the time period 600–14 400 s. In particular, we have now identified the presence of the high (H)- and low (L)-elution components in the split elution bands and have used these bands, which occur in solutions of higher HCl concentration, to elucidate details of the reaction mechanism.

Theoretical background

The generalized 2D correlation theory proposed by Noda^{11,12} has been applied to IR, Raman and near-IR studies.^{13–17} Based on the original concept of 2D spectral analysis, this ver-

satellite theory for data analysis can also be applied to GPC elution profiles.^{9,10}

Dynamic GPC profiles

The time-resolved GPC trace intensity, $I(E, t)$, can be expressed as a function not only of the chromatographic elution time, E , but also the sampling time, t , of a reaction for each aliquot collected during the period between T_{\min} and T_{\max} . The *dynamic GPC trace intensity* $\tilde{y}(E, t)$ of a time-resolved GPC profile is expressed by

$$\tilde{y}(E, t) = \begin{cases} I(E, t) - \bar{I}(E) & \text{for } T_{\min} \leq t \leq T_{\max} \\ 0 & \text{otherwise} \end{cases} \quad (1)$$

where $\bar{I}(E)$ is the *reference GPC trace profile* of the system. The reference trace $\bar{I}(E)$ is set to be the time-average of trace profiles over the observed period.

$$\bar{I}(E) = \frac{1}{T_{\max} - T_{\min}} \int_{T_{\min}}^{T_{\max}} I(E, t) dt. \quad (2)$$

The reference trace could be set simply equal to *zero*; in this case, the dynamic trace is identical to the observed variation of the GPC trace profile. For the present 2D GPC analysis, the conventional form of reference trace defined by eqn. (2) is adopted.

2D correlation for GPC trace

The generalized 2D correlation function^{11,12} for time-resolved GPC analysis is defined as

$$\Phi(E_1, E_2) + i\Psi(E_1, E_2) = \frac{1}{\pi(T_{\max} - T_{\min})} \times \int_0^\infty \tilde{Y}_1(\omega) \cdot \tilde{Y}_2^*(\omega) d\omega. \quad (3)$$

The real and imaginary components of the 2D correlation function, $\Phi(E_1, E_2)$ and $\Psi(E_1, E_2)$, are known, respectively, as the *synchronous* and *asynchronous* 2D correlation intensities. The synchronous 2D correlation intensity $\Phi(E_1, E_2)$ represents the overall similarity or coincidental trends between two separate concentration indicator (*e.g.*, refractive index intensity) variations of the GPC trace measured at different elution counts, as the value of sampling (*i.e.*, reaction) time t is scanned from T_{\min} to T_{\max} . The asynchronous 2D correlation intensity $\Psi(E_1, E_2)$ may be regarded as a measure of dissimilarity or out-of-phase character of the GPC trace intensity variations.

The term, $\tilde{Y}(\omega)$, which is the forward Fourier transform of the dynamic trace intensity variations, $\tilde{I}(E_1, t)$, observed at some given elution count, E_1 , with respect to the sampling time, t , is given by

$$\tilde{Y}_1(\omega) = \int_{-\infty}^{\infty} \tilde{y}(E_1, t) e^{-i\omega t} dt. \quad (4)$$

According to eqn. (1), the above Fourier integration of the dynamic spectrum is actually bound by the finite interval between T_{\min} and T_{\max} . The Fourier frequency, ω , represents the individual frequency component of the variation of $\tilde{I}(E_1, t)$ traced along the sampling time, t . The conjugate of the Fourier transform, $\tilde{Y}_2^*(\omega)$, of the refractive index intensity variation, $\tilde{I}(E_2, t)$, observed at elution time, E_2 , is expressed by

$$\tilde{Y}_2^*(\omega) = \int_{-\infty}^{\infty} \tilde{y}(E_2, t) e^{+i\omega t} dt. \quad (5)$$

Once the appropriate Fourier transformation of the dynamic trace, $\tilde{y}(E, t)$, defined in the form of eqn. (1) is carried out with respect to the sampling time, t , eqn. (3) directly provides the synchronous and asynchronous correlation spectra, $\Phi(E_1, E_2)$

and $\Psi(E_1, E_2)$. The basic properties of generalized 2D correlation spectra are described in detail elsewhere.^{11,12} Further details of synchronous and asynchronous 2D GPC spectra can be also found elsewhere.⁹⁻¹³

Experimental

Materials

1*H*,1*H*,2*H*,2*H*-perfluoro-octyltriethoxysilane (PFOTES, $\text{F}(\text{CF}_2)_6\text{CH}_2\text{CH}_2\text{Si}(\text{OC}_2\text{H}_5)_3$) was purchased from Lancaster Synthesis (UK), and was used without further purification. The PFOTES–ethanol–0.5, 1.0, 2.0 M HCl–H₂O (1 : 1 : 0.4 weight ratio) systems were used as acid-catalyzed reaction mixtures at 298 K.

Time resolved GPC measurements

GPC measurements were carried out using a Shimadzu high-performance liquid chromatography system, which consists of a column oven CTO-10Avp equipped with an Asahipack GF-310HQ column (30 cm) operated at 303 K, a high pressure solvent LC-10Advp delivery pump, a DGU-14A degasser, and an RID-10A refractive index detector. Tetrahydrofuran was used as the eluent at a flow rate of 0.6 ml min⁻¹. The chromatograms were calibrated with polystyrene standards (Shodex STANDARD SL-105). Time resolved GPC profiles were obtained by the following method. Aliquots (0.002 ml) were sampled from the reaction mixture of the PFOES–ethanol–HCl–H₂O systems at various times during steps I and II and were quickly diluted with 1 ml of THF chilled to 273 K. Thus, 40 samples involving time-dependent composition were obtained and analyzed by GPC.

The times for commencement of step II, determined from the near-IR data,¹⁸ were 9300 s for the 0.5 M, 5300 s for the 1.0 M and 2000 s for the 2.0 M HCl–H₂O systems.

2D GPC correlation analysis

Synchronous and asynchronous 2D GPC correlation spectra were calculated from the time-resolved GPC profiles. Computations were carried out using the 2D OGAIZA software, developed at Nagoya Institute of Technology.

Results

Time-resolved GPC profiles

Time and HCl-concentration dependent GPC profiles for the PFOTES–ethanol–HCl–H₂O systems are shown in Fig. 1. Assignment of these elution bands, made on the basis of the GPC profiles of the amino-propyltriethoxysilane and amino-propyltrihydroxysilane systems,⁹ is listed in Table 1. The elution bands A and C, which appear in common at 13.0 and

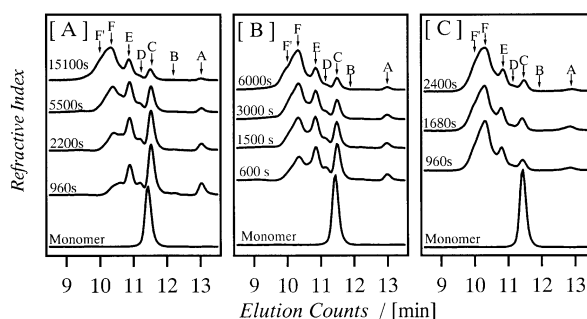


Fig. 1 Time-resolved GPC elution profiles of [A]: 0.5 M, [B]: 1.0 M, [C]: 2.0 M HCl-catalyzed systems.

Table 1 Tentative assignments of elution peaks

Elution counts	Band no.	Tentative assignment
13.0	A	Trihydrolyzed PFOTES (PFOTHS)
12.1 (broad)	B	Dihydrolyzed PFOTES (PFODHS) Monohydrolyzed PFOTES (PFOMHS)
11.5	C	PFOTES + PFOMHS
11.2	D	Component I
10.8	E	Component II
10.5	E'	Component II'
10.3	F	Component III
10.1	F'	Component IV (high molecular weight components)

11.5 counts, respectively, correspond to the perfluoro-octyltri-hydroxysilane (PFOTHS) and PFOTES monomers, respectively. We may assign the extremely weak band B to mono- and di-hydrolyzed silanes (PFOMHS and PFODHS). The bands D, E, F and F', eluted at 11.2, 10.8, 10.3 and 10.1 counts, may be assigned to the polymeric components I, II, III and IV, respectively. Based on the GPC-calibration of polystyrene-standards (M_w : 580–21 900), it is highly probable that components I and II consist of smaller aggregates (SA) and components III and IV of larger aggregates (LA). Furthermore, we assume that the broad shoulder band, F', consists of some weak bands (F'' and F''').

With time, the intensities of bands A and C decrease, while that of band F rapidly increases. This variation indicates that consumption of PFOTHS and PFOTES occurs to form smaller and larger clusters and, as a consequence, the fractions of these species vary with time. As the HCl-concentration increases, the intensities of bands A and C decrease, while that

of band F increases, indicating that high acidity increases the fraction of components III and IV.

It is very difficult to determine the order of variation in relative intensity for all elution peaks in conventional GPC profiles. However, a 2D GPC correlation technique makes this task much simpler and more straightforward.

2D GPC correlation and its time- and HCl-concentration dependence

0.5 M HCl-catalyzed system. The synchronous spectrum in the region of $E_1 = E_2 = 9.5$ –13.3 counts, calculated from the GPC profiles in step I (2700–7000 s) for the 0.5 M HCl system, is shown in Fig. 2[A](a). The signs, coordinates and the correlations ($X \leftrightarrow Y$) of the cross peaks are summarized in Table 2, together with the order of event. The very strong intensity of the autopeak C suggests that the PFOTES monomers are rapidly consumed in the hydrolysis reaction.

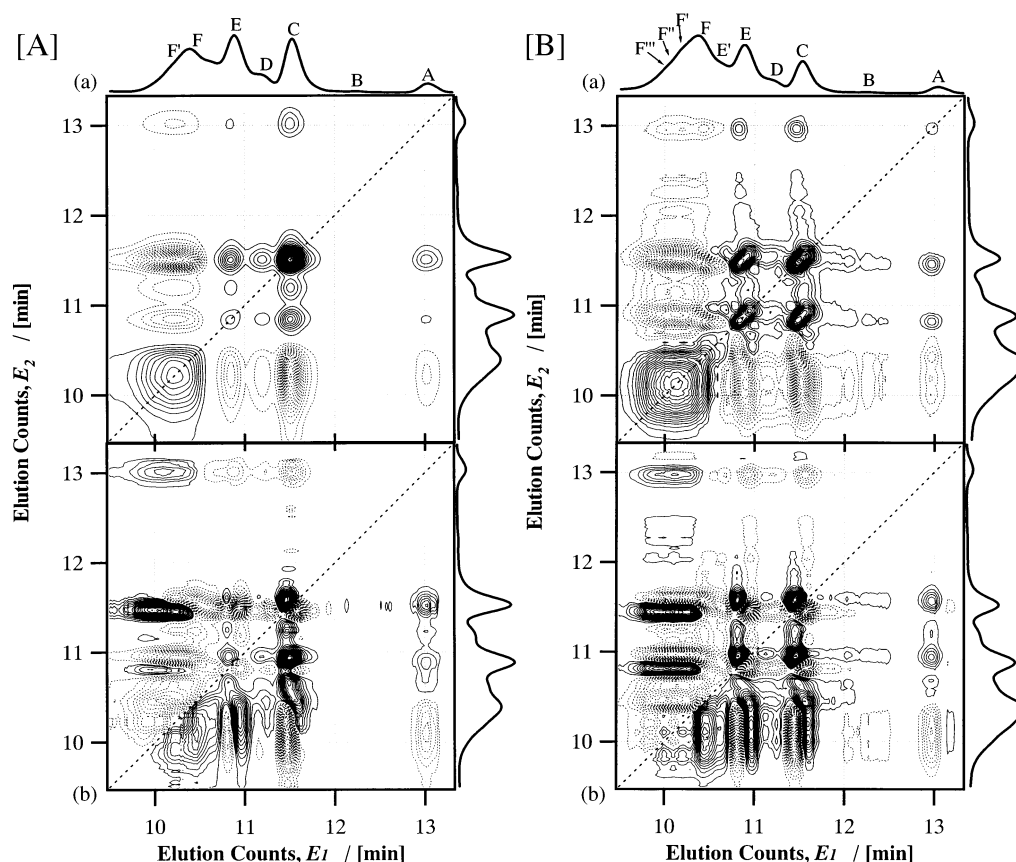


Fig. 2 (a) Synchronous and (b) asynchronous spectra of [A] step I (2700–7000 s) and [B] step II (9120–13320 s) for the 0.5 M HCl-catalyzed sample.

Table 2 Synchronous and asynchronous correlations for the 0.5 M HCl-H₂O- catalyzed system: band correlations, signs and order of events

Step I	Sign ^b		Order of events ^c
	Synchronous (Φ)	Asynchronous (Ψ)	
Correlation ^a			
A _L ↔ C, E(w)	+	+	A _L → C, E
A _L ↔ F, F'(w)	–	–	F, F' → A _L
B ↔ C(w)	+	+	B → C
C _H ↔ C _L (s), D _L (m), E _L (m)	+	–	C _H → C _L , D _L , E _L
C _H ↔ F(s), F'(s)	–	+	F, F' → C _H
C _L ↔ D _H (m), E _H (s)	+	+	C _L → D _H , E _H
C _L ↔ F'(s)	–	–	F' → C _L
D _H , D _L ↔ E _H (w), E _L (s)	+	–	D _H , D _L → E _H , E _L
D _H ↔ F(w), F'(w)	–	+	F, F' → D _H
D _L ↔ F'(w)	–	–	F, F' → D _L
E _H ↔ F(s), F'(s)	–	+	F, F' → E _H
E _L ↔ F'(m)	–	–	F, F' → E _L
Step II			
A _L ↔ C(m), E(w)	+	+	A _L → C, E
A _L ↔ F, F'(w)	–	–	F, F' → A _L
A _H ↔ C(w)	+	–	A _H → C
A _H ↔ F, F'(w)	+	+	A _H → F, F'
B ↔ C, D, E(w)	+	+	B → C, D, E
B ↔ F, F'(w)	–	–	F, F' → B
C _H ↔ D _L (w), E _L (w)	+	–	C _H → D _L , E _L
C _H ↔ E'(s), F(s), F'(s)	–	+	E', F, F' → C _H
C _L ↔ D _H (s), E _H (s)	+	+	C _L → D _H , E _H
C _L ↔ E'(s), F(s), F'(s)	–	–	E', F, F' → C _L
D _H ↔ E _L (m)	+	–	D _H → E _L
D _L ↔ E _H (w)	+	+	D _L → E _H
D _H ↔ E'(w), F(w), F'(w)	–	+	E', F, F' → D _H
D _L ↔ E'(w), F(w), F'(w)	–	+	E', F, F' → D _L
E _H ↔ E _L (m)	+	–	E _H → E _L
E _H ↔ E'(s), F(s), F'(s)	–	+	E', F, F' → E _H
E _L ↔ E'(s), F(s), F'(s)	–	–	E', F, F' → E _L

^a Count number of elution peaks: A_L(13.0), A_H(13.19), B(12.14–12.61), C(11.49), C_H(11.60), C_L(11.45), D_H(11.25), D_L(11.16), E(10.85), E_H(10.95), E_L(10.81), E'(10.67), F(10.35), F'(10.13), and s: strong, m: medium, w: weak. ^b +: positive, –: negative. ^c E_x → E_y: the event of E_x occurs before that of E_y.

The signs of the D ↔ E cross peaks are positive, reflecting the decreasing population of components I and II with time. The two very strong and broad cross peaks with a negative sign, arising from band F, reflect the increasing population of components III and IV with time. The four negative cross peaks, arising from the D ↔ F or E ↔ F (or F') correlations, imply that the condensation reaction or interaction between smaller aggregates brings about components III and IV.

The weak A ↔ C cross peak arises from the fact that the PFOTHS monomers (band A) are produced as a consequence of the hydrolysis reaction of PFOTES monomers (band C). The positive sign of this correlation peak reflects the reduced intensity of band C. The weak A ↔ F cross peak with a negative sign implies that the consumption of PFOTHS monomers brings about formation of components III and IV. Furthermore, band C correlates strongly with bands F and F'.

The asynchronous spectrum (step I) for the same system is shown in Fig. 2[A](b). It is found that each of the four elution bands (C, D, E and F) consists of two components (C_H(high-elution component), C_L(low-elution component), D_H, D_L, E_H, E_L, and F_H and F_L), detected by the resolution enhancing characteristics of the 2D GPC spectra. The two components, C_H and C_L, correlate with two other components, X_H and X_L, respectively. In step I, the C_H ↔ E' (or F or F') correlation brings about at least two cross peaks, while the C_L ↔ F (or F') correlation provides four negative cross peaks. The E_H ↔ F (or

F') and E_L ↔ F' (or F) correlations separately provide asynchronous cross peaks. Thus, elution bands arising from the PFOTES monomer and small aggregates evidently correlate with a set of larger aggregates. These correlations reflect that the reaction or interaction among the monomers and small aggregates brings about larger aggregates. The order of events for these asynchronous correlation peaks is also listed in Table 2.

The synchronous spectrum (step II), calculated from the GPC data collected over a time period of 10 300–15 100 s for the 0.5 M HCl system, is shown in Fig. 2[B](a). Each of the auto and cross peaks arising from bands C and E clearly split into two components (C_H, C_L and E_H, E_L). The very strong intensities of the split cross peaks, as well as those of the split autopeaks, reflect that the population of these components in step II reduces rapidly with time. A very broad and strong autopeak and very broad negative cross peaks, which arise from bands F and F', reflect a rapid increase in population for the III and IV components in step II. Furthermore, we find that the components of bands C and E weakly correlate with the component of band E'.

In the asynchronous spectrum (step II) of the same sample, shown in Fig. 2[B](b), we find a marked splitting of cross peaks arising from elution bands A, C, D, E and E'. The C_H ↔ D_L and C_L ↔ D_H correlations provide the negative and two positive cross peaks, respectively, indicating the existence of a cor-

relation between the monomer and small aggregates. It should also be noted that the A_L and A_H components correlate with the F and F' bands, respectively.

We emphasize the significance of the observation that a strong correlation among the E components, bands E', F and F', in addition to that among the C components, bands F and E', appears in step II. The $C_H \leftrightarrow F$ (or E' or F') correlation provides at least five cross peaks, implying that the correlation between the CH component and these polymerized components becomes stronger than was the case in step I. The $C_L \leftrightarrow F$ (or E' or F') correlation is stronger in step II, compared with that in step I. The two components of bands D and E' correlate strongly with component IV in step II. The order of events for these correlation peaks is also listed in Table 2.

1.0 M HCl-catalyzed system. The synchronous spectrum (step I (1080–2500 s)) for the 1.0 M HCl-H₂O-catalyzed sample is shown in Fig. 3[A](a). The correlation pattern is very similar to that for the synchronous spectrum (step I) for the 0.5 M HCl system. However, the contour levels of the band E autop-peak and of the positive C (or D) \leftrightarrow E cross peaks are higher than those in the synchronous spectrum (step I) for the 0.5 M HCl system. This observation reflects the greater intensity reduction of bands C, D and E. The negative cross peaks of the E \leftrightarrow F' (or F) correlation increase in intensity, reflecting the marked increase in contour level promoted by a higher HCl-concentration.

The signs of the correlation peaks in the synchronous spectrum (step I) for the 1.0 M HCl system are the same as those in the synchronous spectrum (step I) for the 0.5 M HCl system. However, the cross peaks in the asynchronous spectrum (step I) for the 1.0 M HCl-catalyzed system (Fig. 3[A](b), listed in Table 3) furnish the opposite sign: for example, the sign of the $C_H \leftrightarrow C_L$ cross peak is negative in the asynchronous spectrum (step I) for the 0.5 M HCl system, while that of the same

cross peak for the 1.0 M HCl system in the asynchronous spectrum (step I) is positive. According to the sign rules established for 2D correlation spectra,¹² this result implies that the event giving rise to the cross peak with opposite sign in the 1.0 M HCl-system occurs in the same manner as that in the 0.5 M HCl-system. The order of events corresponding to the individual cross peaks is listed in Table 3.

From the resolution-enhancing characteristics of the asynchronous correlation, it has also been confirmed that each of elution bands A, C, D and E splits into L- and H-components. Band F splits into two components and correlates with band F' and higher molecular weight components (F'', or F''').

In the synchronous spectrum (step II (3200–5800 s)), (Fig. 3[B](a)), the density of the contour levels for each of the correlation peaks becomes higher, compared with that for step II in the 0.5 M HCl system. Finally, each correlation region is clearly segregated, reflecting the rapid growth of the large aggregates. Two positive regions (SA region (C, D and E) and LA region (E', F, F' and F'')) appear, containing autop- peaks and negative cross peak regions, and the LA region is particularly intense.

In the asynchronous spectrum (step II, Fig. 3[B](b)) for the 1.0 M HCl system, the spectral feature in the region $E_1 = E_2 = 10.5 - 13.3$ (SA region) is very similar to that in the same region for step II in the 0.5 M HCl system. However, in the regions $E_1 = 9.5 - 13.3$ and $E_2 = 9.5 - 10.5$, the cross peaks, which arise from the $C_H \leftrightarrow E'$, $E_H \leftrightarrow F$ (or F') and $E' \leftrightarrow F$ (or F') correlations, abruptly increase in intensity, again reflecting the rapid growth of larger aggregates.

2.0 M HCl-catalyzed system. Fig. 4[A](a) shows the synchronous spectrum (step I (950–1850 s)) for the 2.0 M HCl-catalyzed system. The band correlations and order of events are listed in Table 4. In addition to the two autop- peaks and two cross peaks arising from the $C_L \leftrightarrow E_L$ correlation, two very

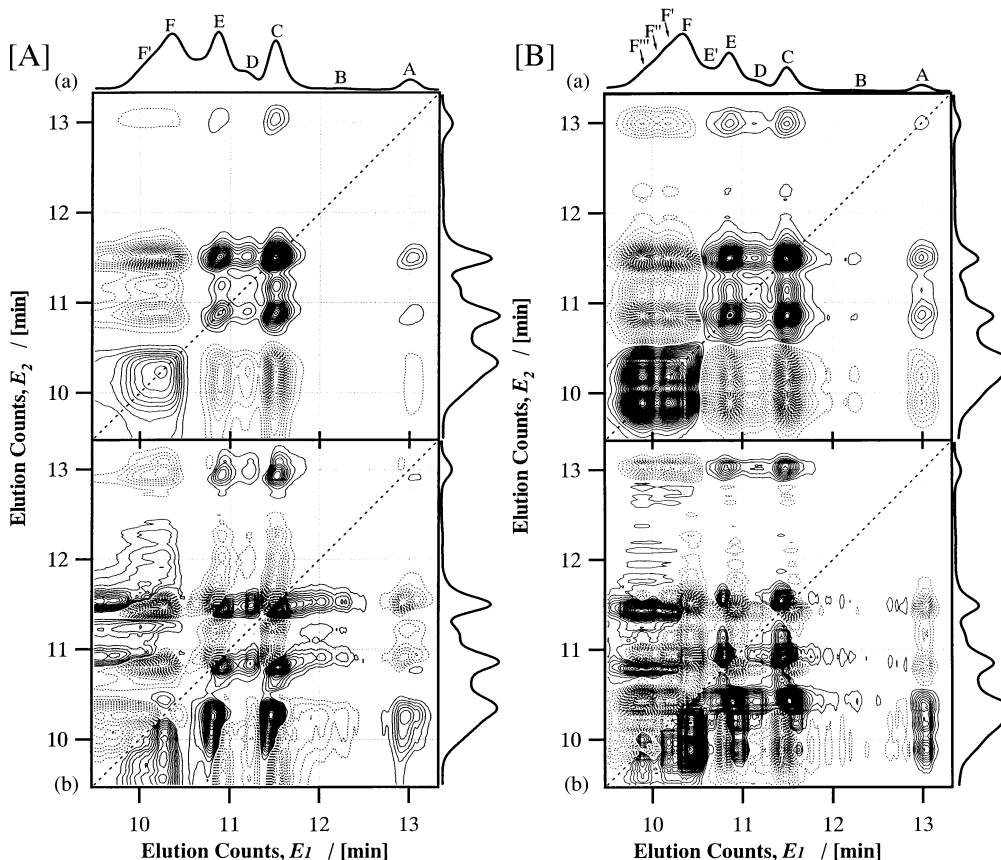


Fig. 3 (a) Synchronous and (b) asynchronous spectra of [A] step I (1100–2520 s) and [B] step II (3200–5880 s) for the 1.0 M HCl-catalyzed sample.

Table 3 Synchronous and asynchronous correlations for the 1.0 M HCl-H₂O-catalyzed system – band correlations, signs and order of events

Step I			
Correlation ^a	Sign		Order of events
	Synchronous (Φ)	Asynchronous (Ψ)	
A _L , A _H ↔ C(w), D(w), E _H (w)	+	–	A _L , A _H → C, D, E _H
A _L , A _H ↔ E _L (w)	+	+	A _L , A _H → E _L
A _L , A _H ↔ F(w), F'(w)	–	+	E', F, F' → A _L , A _H
B ↔ C(w), D(w), E(w)	+	+	B → C, D, E
B ↔ F(w), F'(w)	+	–	B → F, F'
C _H ↔ C _L (s), E _L (s)	+	+	C _H → C _L , E _L
C _H ↔ F'(s)	–	–	F' → C _H
C _L ↔ D _H (m), E _H (s)	+	–	C _L → D _H , E _H
C _L ↔ F(s), F'(s)	–	+	F, F' → C _L
D _H ↔ E _H (m)	+	+	D _H → E _H
D _H ↔ F(m), F'(m)	–	–	F, F' → D _H
E _H ↔ E _L (m)	+	+	E _H → E _L
E _H ↔ F, F'(m)	–	–	F, F' → E _H
E _L ↔ F(s), F'(s)	–	+	F, F' → E _L
F ↔ F'(m)	+	+	F → F'
Step II			
A _L ↔ C(m), D(m), E _H (m), E _L (m)	+	–	A _L → C, D, E _H , E _L
A _L ↔ E'(m), F(m), F'(m)	–	+	E', F, F' → A _L
B ↔ C(w), E _H (w), E _L (w)	+	+	B → C, E _H , E _L
B ↔ E'(w)	–	+	E' → B
B ↔ F, F'(w)	–	–	F, F' → B
C → E'(s)	–	+	E' → C
C _H ↔ C _L (s), D _H (w), E _L (m)	+	–	C _H → C _L , D _H , E _L
C _L ↔ D _L (s), E _H (s)	+	+	C _L → D _L , E _H
C _L ↔ F(s), F'(s)	–	–	F, F' → C _L
D _L ↔ E _L (m)	+	–	D _L → E _L
D _L ↔ E'(m)	–	+	E' → D _L
D _L ↔ F'(w)	–	+	F' → D _L
E _H ↔ E _L (s)	+	–	E _H → E _L
E _L ↔ F(s), F'(s)	–	+	F, F' → E _H
E _H ↔ F(s), F'(s)	–	–	F, F' → E _H
E' ↔ F(s), F'(s)	+	+	E' → F, F'
F' ↔ F''(m)	+	+	F' → F''

^a Count number of elution peaks: A_L(12.95), A_H(13.09), B(12.01–12.40), C(11.53), C_H(11.57), C_L(11.45), D(11.21), D_H(11.24), D_L(11.13), E(10.91), E_H(10.93), E_L(10.80), E'(10.66), F(10.33), F'(9.89), and *s*: strong, *m*: medium, *w*: weak.

strong autopeaks arising from bands E' and F' appear in the region $E_1 = E_2 = 9.5 - 10.5$ (larger aggregate region), implying that bands E' and F' rapidly increase in intensity with time in step I. The negative cross peaks come from correlation of bands E', F and F' with bands C_L and E_L (or E'). The very strong intensities of these cross peaks must reflect that bands for the polymeric aggregates, which strongly correlate with bands E', F and F', rapidly increase in intensity as a consequence of interaction of the C_L and E_L components.

We find that the components A_L and A_H correlate with band C_L (or E_L), providing the fused-type cross peak with two maxima. It seems that correlation of the A_L and A_H components with bands E', F and F' provides the negative cross peaks.

The asynchronous spectrum (step I) of the 2.0 M HCl system is shown in Fig. 4[A](b). The correlations between pairs of bands are also listed in Table 3. In the regions $E_1 = 9.5 - 13.3$ and $E_2 = 9.5 - 10.5$, the correlation of bands C_L with bands E' and F' provides two cross peaks at coordinate (11.39, 10.37) and (11.39, 10.03). In the same region, the correlation of band E_L with bands E' and F' also provides two cross peaks at coordinates (10.75, 10.37) and (10.75, 10.03). These correlations reveal that the C_L (or E_L) component is consumed to form the high molecular weight component F'.

Fig. 4[B](a) shows the synchronous spectrum (step II (2040–2400 s)) for the 2.0 M HCl system. In the SA region, the autop-

peaks and cross peaks, derived from each of the C_H, C_L, E_H and E_L components, are very clearly segregated. The C_H ↔ C_L correlation provides two autopeaks and two negative cross peaks which construct a small correlation square. Since we may assume the existence of a very weak autopeak arising from component E_L, we may construct a small correlation square by connecting the E_H and E_L autopeaks with two negative cross peaks. Furthermore, it may be assumed that the E'_H ↔ E'_L correlation provides two autopeaks and two positive cross peaks, which may also be constructed into a small correlation square. When we compare the intensity of the C_H (or E_H) autopeak with that of the C_L (or E_L) autopeak, we find that the intensity of the C_H (or E_H) autopeak is greater than that of the C_L (or E_L) autopeak. This fact implies that the C_H (or E_H) component contributes to a major extent to the polymerization process in this region. In particular, the very strong intensity of the E_H autopeak suggests that the E_H component is rapidly consumed by reaction or interaction in step I.

In the LA region, four autopeaks and at least six positive cross peaks, derived from bands F, F' and other bands, probably reflect the rapid production of these polymeric aggregates, as a consequence of reaction or interaction among the components of C, D, E and E'. We note that at least three very small correlation squares exist in this region.

The C_H ↔ E_H, C_H ↔ E' and E_H ↔ E' correlations bring about very strong positive cross peaks, while the C_L ↔ E_H,

Table 4 Synchronous and asynchronous correlations for the 2.0 M HCl·H₂O-catalyzed system—band correlations, signs and order of events

Step I			
	Sign		
Correlation ^a	Synchronous (Φ)	Asynchronous (Ψ)	Order of events
$A \leftrightarrow C(m)$, $E_H(m)$	+	—	$A \rightarrow C$, E_H
$A \leftrightarrow E'(m)$, $F(m)$, $F'(m)$	—	+	E' , F , $F' \rightarrow A$
$C_H \leftrightarrow C_L(w)$, $E_L(w)$	+	+	$C_H \rightarrow C_L$, E_L
$C_H \leftrightarrow E'(s)$, $F'(s)$	—	—	E' , $F' \rightarrow C_H$
$C_L \leftrightarrow E_H(m)$	+	—	$C_L \rightarrow E_H$
$C_L \leftrightarrow F'(s)$	—	+	$F' \rightarrow C_L$
$D_H \leftrightarrow F(w)$	—	—	$F \rightarrow D_H$
$D_L \leftrightarrow F'(w)$	—	+	$F' \rightarrow D_L$
$E_L \leftrightarrow F(s)$	—	—	$F \rightarrow E_L$
$E_L \leftrightarrow F'(s)$	—	+	$F' \rightarrow E_L$
Step II			
$A \leftrightarrow C(w)$, $E(w)$, $E'(w)$	—	—	$A \rightarrow C$, E , E'
$A \leftrightarrow F(w)$, $F'(w)$	+	+	$A \rightarrow F$, F'
$C_H \leftrightarrow C_L(w)$, $E_L(w)$, $F(s)$, $F'(s)$	—	+	C_L , E_L , F , $F \rightarrow C_H$
$C_H \leftrightarrow D_H(w)$, $E_H(s)$	+	—	$C_H \rightarrow D_H$, E_H
$C_H \leftrightarrow E'(s)$	+	+	$C_H \rightarrow E'$
$C_H \leftrightarrow F''(s)$	—	—	$F'' \rightarrow C_H$
$C_L \leftrightarrow D_H(w)$, $E_H(m)$, $E'(m)$	—	—	D_H , E_H , $E' \rightarrow C_L$
$C_L \leftrightarrow F(m)$	+	—	$C_L \rightarrow F$
$C_L \leftrightarrow F'(m)$, $F''(m)$	+	+	$C_L \rightarrow F'$, F''
$D_H \leftrightarrow E'(w)$	+	+	$D_H \rightarrow E'$
$E_H \leftrightarrow E_L(w)$	—	+	$E_L \rightarrow E_H$
$E_H \leftrightarrow E'(s)$	+	+	$E_H \rightarrow E'$
$E_H \leftrightarrow F(s)$	—	+	$F \rightarrow E_H$
$E_L \leftrightarrow E'(w)$	—	—	$E' \rightarrow E_L$
$E_L \leftrightarrow F(w)$, $F''(w)$	+	+	$E_L \rightarrow F$, F''
$E' \leftrightarrow F(s)$	—	+	$F \rightarrow E'$

^a Count number of elution peaks: A(12.75), B(12.02–12.4), C(11.53), C_H(11.57), C_L(11.37), D_H(11.13), D_L(11.09), E_H(10.90), E_L(10.75), E'(10.42), F(10.26), F'(9.89), and s: strong, m: medium, w: weak.

^a Count number of elution peaks: A(12.75), B(12.02–12.4), C(11.53), C_H(11.57), C_L(11.37), D_H(11.13), D_L(11.09), E_H(10.90), E_L(10.75), E'(10.42), F(10.26), F'(9.89), and *s*: strong, *m*: medium, *w*: weak.

$C_L \leftrightarrow E'$ and $E_L \leftrightarrow E'$ correlations provide negative cross peaks with lower intensities, also reflecting the marked consumption of the C_H and E_H components in step II.

The correlation of the C_H or E_H components with bands F, F' and F'' results in the appearance of very strong and negative cross peaks, reflecting that these components are rapidly consumed in step II to form polymeric aggregates. The correlation of the C_L or E_L components with bands F, F' and F'' provides relatively weak and positive cross peaks, implying that consumption of these components to form polymeric components is not extensive.

In the regions $E_1 = 12.5 - 13.3$ and $E_2 = 9.5 - 13.3$, for the synchronous spectrum (step II) of the 2.0 M HCl system, we find three cross peaks, arising from $A_L \leftrightarrow C_H$, $A_L \leftrightarrow E_H$ and $A_L \leftrightarrow E'$ correlations, as well as cross peaks from the $A_L \leftrightarrow F$ (or F' or F'') correlations. The signs of the three former peaks are negative, while those of the latter peaks and the F, F' and F'' bands increase in intensity.

The asynchronous spectrum (step II) for the same sample is shown in Fig. 4[B](b). The distribution of the cross peaks with very high contour levels is concentrated in the regions $E_1 = 9.5 - 13.3$ and $E_2 = 9.5 - 11.0$. Enhancement of the spectral resolution brings about clear separation of the cross peaks for the correlations among the L- and H-components of bands C, E and E', and bands F and F'. That is, correlations between smaller and larger aggregates are dominant in these overlapping regions.

In particular, in the regions $E_1 = 9.5 - 13.3$ and $E_2 = 9.5 - 10.5$, the cross peaks are clearly separated; moreover, their contour levels are much higher than those in the asynchronous spectrum (step II) for the 1.0 M HCl-system,

reflecting the strong correlation between smaller aggregates and the formation of larger aggregates. The $C_H \leftrightarrow F$, $E_H \leftrightarrow F$ and $E' \leftrightarrow F$ correlations provide a positive cross peak with extremely high contour levels, indicating that the C_H-, E_H-components and the E' band strongly correlate with formation of the component of band F. Furthermore, in the region $E_2 = 9.5 - 10.0$ counts, the C_H (or E_H) \leftrightarrow F' correlation provides at least three broad negative cross peaks with relatively high contour levels, while the C_L (or E_L) \leftrightarrow F' correlation provides at least three positive cross peaks with relatively high contour levels. It is also found that the F \leftrightarrow F' correlation brings about clear positive cross peaks with high intensity.

Discussion

The 2D GPC correlation spectra, calculated from the time-resolved GPC profiles collected over a time-period of 10–240 min, provide direct information on the dynamic variation of the sequence of intricate reactions or interactions in polymerization. We may now summarize the correlations among the elution bands which were obtained in the synchronous spectra (steps I and II), as follows (Fig. 5). In Fig. 5, the thick, intermediate and thin biarrows indicate very strong, strong and weak band correlations, respectively.

Step I: (1) For the 0.5 and 1.0 M HCl systems, the very strong $C \leftrightarrow F$ (or F') correlation is dominant, although weak or intermediate $C \leftrightarrow D$, $C \leftrightarrow E$ and $C \leftrightarrow F$ (or F') correlations also exist (Fig. 5[A] (a) and (b)). (2) For the 2.0 M HCl system, the very strong $C \leftrightarrow F$ (or F') and $E \leftrightarrow F$ (or F') correlations

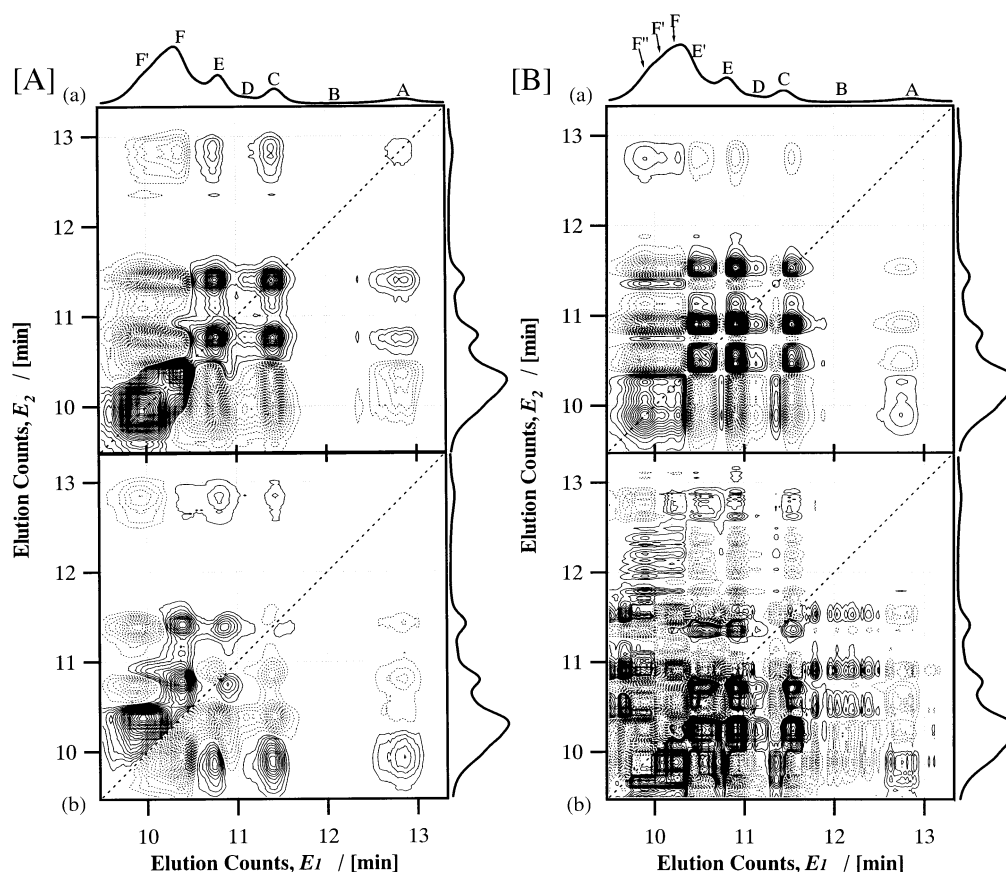


Fig. 4 (a) Synchronous and (b) asynchronous spectra of [A] step I (960–1860 s) and [B] step II (2000–2400 s) for the 2.0 M HCl-catalyzed sample.

appear, in addition to the weak $C \leftrightarrow D$ and $C \leftrightarrow E$ correlations (Fig. 5[A] (c)).

Step II: (1) For the 0.5 M HCl system, bands C and E split clearly into two components (L- and H-components, C_L and C_H , E_L and E_H). Each of these components weakly correlates with other bands or components. (2) For the 2.0 M HCl system, the very strong correlations of the L- and H-components of C, E, and E' with F (or F' or F'') appear. In particular, correlations between the H-H-components are dominant.

Thus, in step I, small aggregates (C, D and, in particular E) grow up to form large aggregates (F and F'). A high HCl concentration promotes the growth process from component II (E) to components III (F) and IV (F'). In step II, the growth of large aggregates (E' , F, F' and F'') becomes dominant. As the HCl concentration increases, the reaction or interaction among some higher polymerized aggregates (F, F' and F'') becomes stronger. We emphasize that each elution band (C, D and E) splits into two components (L- and H-) in step II (Figure 2[B]). The high HCl concentration evidently promotes this splitting and strengthens the correlations among these L- and H-components. It should be noted that, in step II for the 2.0 M HCl system, the correlations of the C_H and E_H components with large aggregate bands (E' , F, F' and F'') are more dominant than those of the L-components.

Resolution-enhancing characteristics of the asynchronous correlation provide ample evidence for the existence of the L- and H-components and for the component-component correlations (Fig. 4[B]).

The predominant correlations of the H-components with large aggregate bands (E' , F, F' and F'') probably arise from the difference in reactivity between the L- and H-components. The following four assumptions were made, in order to explain this difference.

(1) For the SiOH groups of PFOTHS, which were produced by hydrolysis of PFOTES, formation of associated SiOH

groups may be possible,⁸ leading to the difference in reactivity. Most of the silanol groups, which belong to the associated SiOH groups, probably form a hydrogen-bonding network with SiOH itself, or ethanol or water molecules.⁸ The silanols associated with SiOH are more reactive than those associated with ethanol or water.

(2) A PFOTES molecule easily forms the solvated-type complex $(R_1Si(OEt)_3(OH)_m)_{m-3}$ in ethanol (EtOH).¹⁹ Therefore, in ethanol, the PFOTES molecules are not only in the monomolecular state but also in the complex.

(3) Formation of oligomers with the $Si(OH)(OEt)$ or $Si(OH)_2$ groups may be possible.¹⁹ The reactivity of an oligomeric molecule with unreacted ethoxy groups is smaller than that of the oligomer without ethoxy groups.

(4) The steric hindrance of the bulky perfluoro-octyl chain promotes isolation of any silanol groups which may be incorporated into the grooves of the aggregates of the perfluoro-octyl chains. This may bring about formation of the weakly associated silanols.⁸ This isolation effect probably makes the aggregates less reactive.

Splitting of band A into A_L and A_H components may be explained by assumption (1). Component A_L is probably composed of the PFOTHS molecules solvated by ethanol, while unsolvated PFOTHS molecules constitute component A_H . Band C splits into the C_L and C_H components, a conclusion consistent with assumption (2). In particular, assumption (3) may make a dominant contribution to the splitting (E_L and E_H) of band E (that is, the appearance of E_H as the major component). The isolation effect on the silanols, described in assumption (4), may increase the fractions of the less reactive L-components for bands D, E and E' .

Existence of the L- and H-components is also possible for larger aggregate bands (and probably for all elution bands). In fact, in the asynchronous maps (step II), (Fig. 2[B] and 3[B]), for the 0.5 and 1.0 M HCl systems, we can confirm split-

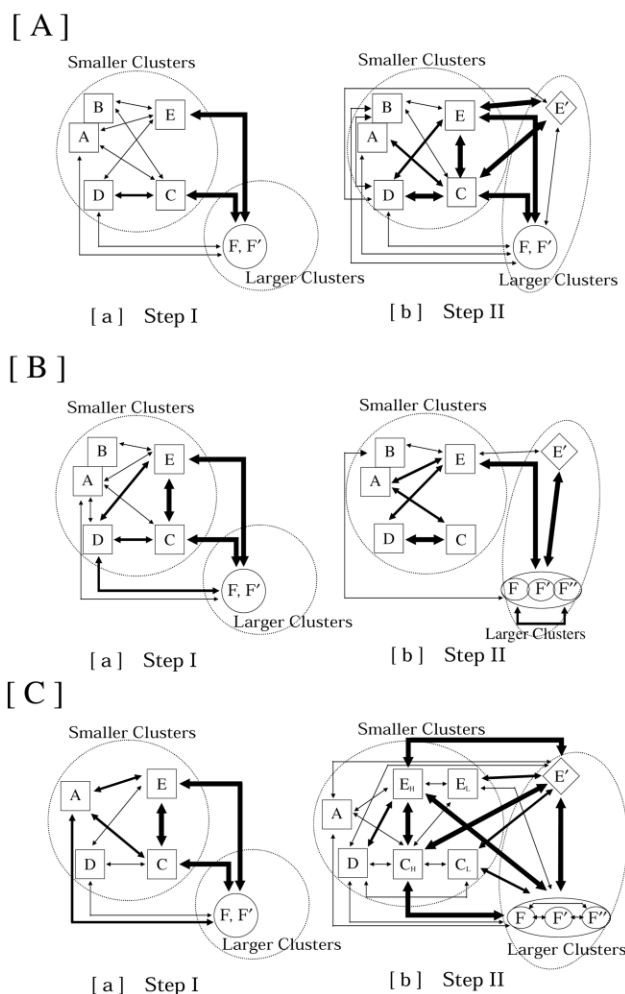


Fig. 5 The correlative diagrams among smaller and larger components for [A] 0.5 M HCl-, [B] 1.0 M HCl-, and [C] 2.0 M HCl-systems. (a): step I and (b): step II.

ting of the F, F', F'' and F''' bands in the region $E_1 = E_2 = 9.5 - 10.5$. In particular, in the asynchronous map (step II) (Fig. 4[B]), for the 2.0 M HCl system, the splitting features of the F' and F'' bands are clearly seen.

In our previous paper,²⁰ we suggested that the strong correlation between the PFOTES monomeric band and the polymeric aggregate band may imply the existence of aggregates of self-assembled perfluoro-octyl chains in the reaction mixture. Recently, we have examined the time-resolved SAXS curves of the same sample system.²¹ The results have shown that the PFOTES molecules form dimeric aggregates in ethanol at zero reaction time. This result supports assumption (4). Accordingly, the correlation of band C with the bands coming from small aggregates and polymeric aggregates may imply the formation of the aggregates, self-assembled through the hydrophobic and lipophobic properties of the perfluoro-octyl chains.

In the present study, no discussion of the correlations of band B with other bands have been made, since the intensity of this elution band is too weak to be useful in the 2D GPC correlation analysis. However, the correlation between band B and other bands may provide significant information on the mechanism for formation of the L- and H-components, since band B may consist of at least two partially hydrolyzed silanes (PFOMHS and PFODHS).

For the growth of the polymer aggregates formed by PFOTES monomers, we have surmised that formation of small aggregates occurs mainly in step I, while in step II larger polymeric aggregates are produced rapidly. Finally, we suggest that this rapid growth in step II may be caused by the appearance of reactive H-components and by the correlation of these predominant H-components with other bands.

Conclusions

The polymerization process (in particular, steps I and II) of the PFOTES-ethanol system, catalyzed by 0.5, 1.0 and 2.0 M HCl-H₂O, has been explored in detail by the use of 2D GPC correlation analysis. The results have demonstrated that features in the 2D GPC correlation spectra directly reflect the dynamic variation in the sequence of intricate reactions or interactions and the differences between steps I and II. We have found that each of the elution bands in step II splits into two major components (reactive H- and nonreactive L-components), and that a high HCl concentration promotes this splitting and the predominant H-component vs. other band correlations. The appearance of the reactive H-components probably induces rapid growth of the polymeric aggregates in step II.

References

- 1 R. K. Iler, *The Chemistry of Silica*, Wiley, New York, 1979.
- 2 E. F. Vansant, P. Van Der Voort and K. C. Vrancken, *Characterization and Chemical Modification of the Silica Surface*; Elsevier, New York, 1995.
- 3 S. Sakka and K. Kamiya, *J. Non-Cryst. Solids*, 1982, **48**, 31.
- 4 K. Nakanishi, N. Soga, H. Matsuoka and N. Ise, *J. Am. Ceram. Soc.*, 1992, **75**(4), 971.
- 5 K. J. Lee, T. Y. Tien and E. Gulari, *J. Non-Cryst. Solids*, 1994, **171**, 46.
- 6 Q. Huo, D. I. Margolese, U. Cliesla, P. Teng, T. E. Gier, P. Sieger, R. Leon, P. M. Petroff, F. Schüth and G. D. Stucky, *Nature*, 1994, **368**, 317.
- 7 T. Ogasawara, K. Izawa, N. Hattori, H. Okabayashi and C. J. O'Connor, *Colloid. Polym. Sci.*, 2000, **278**, 293.
- 8 T. Ogasawara, A. Nara, H. Okabayashi, E. Nishio and C. J. O'Connor, *Colloid Polym. Sci.*, 2000, **278**, 946.
- 9 K. Izawa, T. Ogasawara, H. Masuda, H. Okabayashi and I. Noda, *PhysChemComm*, 2001, **12**.
- 10 I. Noda, *Appl. Spectrosc.*, 1993, **47**, 1329.
- 11 K. Izawa, T. Ogasawara, H. Masuda, H. Okabayashi and I. Noda, *Macromolecules*, 2002, **35**, 92.
- 12 I. Noda, A. E. Dowrey, C. Marcott, G. M. Story and Y. Ozaki, *Appl. Spectrosc.*, 2000, **54**, 236A.
- 13 I. Noda, *Appl. Spectrosc.*, 1990, **44**, 550.
- 14 N. L. Sefara, N. P. Magtoto and H. H. Richardson, *Appl. Spectrosc.*, 1997, **51**, 536.
- 15 I. Noda, Y. Liu, Y. Ozaki and M. Czarnecki, *J. Phys. Chem.*, 1995, **99**, 3068.
- 16 Y. Ren, M. Shimoyama, T. Ninomiya, K. Matsukawa, H. Inoue, I. Noda and Y. Ozaki, *J. Phys. Chem. B*, 1999, **103**, 6475.
- 17 T. Ogasawara, A. Nara, H. Okabayashi, E. Nishio and C. J. O'Connor, *Colloid Polym. Sci.*, 2000, **278**, 1070.
- 18 K. Izawa, T. Ogasawara, H. Masuda, H. Okabayashi, C. J. O'Connor and I. Noda, *Colloid. Polym. Sci.*, 2002, in press.
- 19 H. Einaga, *Inorganic Synthesis in Solution as a Reaction Field*, Baifukan, Tokyo, 2000, p. 169.
- 20 K. Izawa, T. Ogasawara, H. Okabayashi, H. Masuda, C. J. O'Connor and I. Noda, *J. Phys. Chem. B*, 2002, in press.
- 21 K. Izawa, T. Ogasawara, H. Masuda, H. Okabayashi, M. Monkenbusch and C. J. O'Connor, *Colloid Polym. Sci.*, 2002, in press.